

Modelling and Identification of Immune Cell Migration during the Inflammatory Response

PhD Viva (extended version)

A. Kadochnikova¹

¹Department of Automatic Control and Systems Engineering
The University of Sheffield

June 24, 2019



Outline

- 1 Background & Motivation
- 2 Environment inference: homogeneous cell behaviour
- 3 Environment inference: heterogeneous cell behaviour
- 4 Estimating cell morphodynamics
- 5 Conclusion



Experimental studies

Mathematical models



Experimental studies

Recruitment
via chemotaxis

Mathematical models



Experimental studies

Recruitment
via chemotaxis

in vivo microscopy
on zebrafish larvae

Mathematical models



Experimental studies

Recruitment
via chemotaxis

in vivo microscopy
on zebrafish larvae

Resolution via
reverse migration

Mathematical models



Experimental studies

Recruitment
via chemotaxis

in vivo microscopy
on zebrafish larvae

Resolution via
reverse migration

Sensing to motion
via subcellular signals

Mathematical models



Experimental studies

Recruitment
via chemotaxis

in vivo microscopy
on zebrafish larvae

Resolution via
reverse migration

Sensing to motion
via subcellular signals

Mathematical models

RDS models
for populations



Experimental studies

Recruitment
via chemotaxis

in vivo microscopy
on zebrafish larvae

Resolution via
reverse migration

Sensing to motion
via subcellular signals

Mathematical models

RDS models
for populations

Random walk models
for single cells



Experimental studies

Recruitment
via chemotaxis

in vivo microscopy
on zebrafish larvae

Resolution via
reverse migration

Sensing to motion
via subcellular signals

Mathematical models

RDS models
for populations

Random walk models
for single cells

RDS models for
subcellular species



Experimental studies

Recruitment
via chemotaxis

in vivo microscopy
on zebrafish larvae

Resolution via
reverse migration

Sensing to motion
via subcellular signals

Mathematical models

RDS models
for populations

Random walk models
for single cells

RDS models for
subcellular species

Morphodynamics as
intermediate level



Experimental studies

Recruitment
via chemotaxis

in vivo microscopy
on zebrafish larvae

Resolution via
reverse migration

Sensing to motion
via subcellular signals



Mathematical models

RDS models
for populations

Random walk models
for single cells

RDS models for
subcellular species

Morphodynamics as
intermediate level



Experimental studies

Recruitment
via chemotaxis

!!!

Environment
unobserved

Resolution via
reverse migration

Sensing to motion
via subcellular signals

Mathematical models

RDS models
for populations

Random walk models
for single cells

RDS models for
subcellular species

Morphodynamics as
intermediate level



Experimental studies

Recruitment
via chemotaxis

!!!

Environment
unobserved

Random walk
or fugetaxis?

Sensing to motion
via subcellular signals

Mathematical models

RDS models
for populations

Random walk models
for single cells

RDS models for
subcellular species

Morphodynamics as
intermediate level



Experimental studies

Recruitment
via chemotaxis

!!!

Environment
unobserved

Random walk
or fugetaxis?

Sensing to motion
via subcellular signals

Mathematical models

RDS models
for populations

RWs do not reflect
global environment

RDS models for
subcellular species

Morphodynamics as
intermediate level



Experimental studies

Recruitment
via chemotaxis

!!!

Environment
unobserved

Random walk
or fugetaxis?

Sensing to motion
via subcellular signals

Mathematical models

RDS models
for populations

RWs do not reflect
global environment

RDS models for
populations
Models not
informed by
experimental data
at intermediate level



Common concept:
Complicated model → Realistic simulations.



Systematic approach:
Simplified models → Linking to data → Meaningful predictions.



Systematic approach:

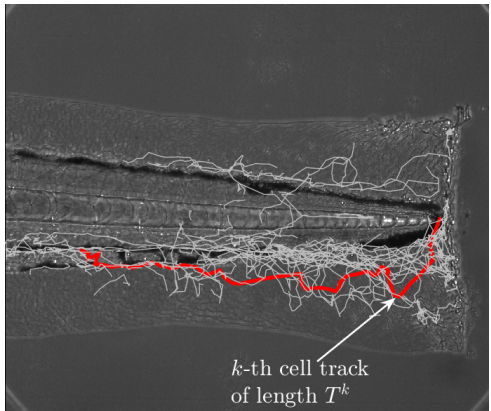
Simplified models → Linking to data → Meaningful predictions.

Objectives:

- Develop a dynamical model that describes cell interaction with the global environment.
- Data-driven estimation of global chemoattractant concentration and cell behavioural modes.
- Parameter estimation of neutrophil morphodynamics model.



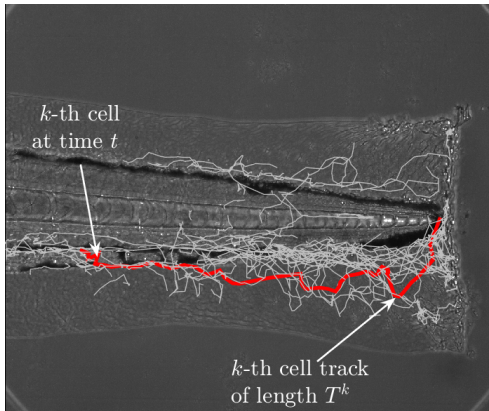
Hidden chemoattractant



Time series data:

- **K tracks:** $\mathcal{Y} = \{\mathbf{y}^k\}_{k=1}^K$
- Single track:
 $\mathbf{y}^k = \{\mathbf{y}_t^k\}_{t=1}^{T^k}$
- Single data point:
 $\mathbf{y}_t^k = [\bar{s}_x, \bar{s}_y]^\top$
- Full state:
 $\mathbf{x}_t^k = [s_x, s_y, v_x, v_y]^\top$
- Environment influence:
 $\mathbf{u}_t^k = \mathbf{u}_t^k(s) = \nabla \mathcal{U}(s)$.

Hidden chemoattractant

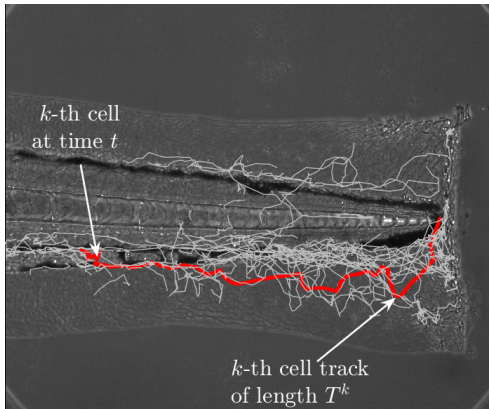


Time series data:

- **K tracks:** $\mathcal{Y} = \{\mathbf{y}^k\}_{k=1}^K$
- **Single track:**
 $\mathbf{y}^k = \{\mathbf{y}_t^k\}_{t=1}^{T^k}$
- **Single data point:**
 $\mathbf{y}_t^k = [\bar{s}_x, \bar{s}_y]^\top$
- **Full state:**
 $\mathbf{x}_t^k = [s_x, s_y, v_x, v_y]^\top$
- **Environment influence:**
 $u_t^k = u_t^k(s) = \nabla \mathcal{U}(s)$.



Hidden chemoattractant

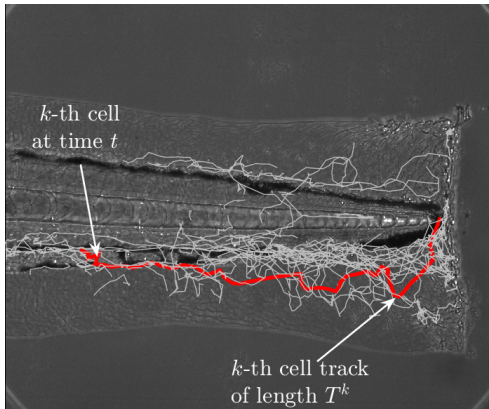


Time series data:

- **K tracks:** $\mathcal{Y} = \{\mathbf{y}^k\}_{k=1}^K$
- **Single track:**
 $\mathbf{y}^k = \{\mathbf{y}_t^k\}_{t=1}^{T^k}$
- **Single data point:**
 $\mathbf{y}_t^k = [\bar{s}_x, \bar{s}_y]^\top$
- **Full state:**
 $\mathbf{x}_t^k = [s_x, s_y, v_x, v_y]^\top$
- **Environment influence:**
 $u_t^k = u_t^k(s) = \nabla \mathcal{U}(s)$.



Hidden chemoattractant

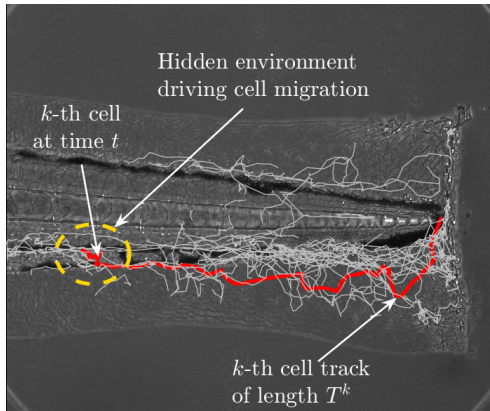


Time series data:

- **K tracks:** $\mathcal{Y} = \{\mathbf{y}^k\}_{k=1}^K$
- **Single track:**
 $\mathbf{y}^k = \{\mathbf{y}_t^k\}_{t=1}^{T^k}$
- **Single data point:**
 $\mathbf{y}_t^k = [\bar{s}_x, \bar{s}_y]^\top$
- **Full state:**
 $\mathbf{x}_t^k = [s_x, s_y, v_x, v_y]^\top$
- **Environment influence:**
 $u_t^k = u_t^k(s) = \nabla \mathcal{U}(s)$.



Hidden chemoattractant

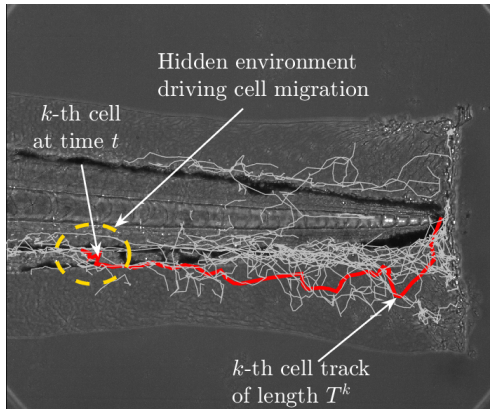


Time series data:

- **K tracks:** $\mathcal{Y} = \{\mathbf{y}^k\}_{k=1}^K$
- **Single track:**
 $\mathbf{y}^k = \{\mathbf{y}_t^k\}_{t=1}^{T^k}$
- **Single data point:**
 $\mathbf{y}_t^k = [\bar{s}_x, \bar{s}_y]^\top$
- **Full state:**
 $\mathbf{x}_t^k = [s_x, s_y, v_x, v_y]^\top$
- **Environment influence:**
 $\mathbf{u}_t^k = \mathbf{u}_t^k(\mathbf{s}) = \nabla \mathcal{U}(\mathbf{s}).$



Hidden chemoattractant



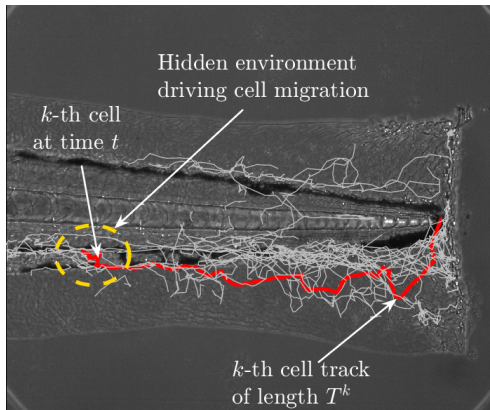
Time series data:

- **K tracks:** $\mathcal{Y} = \{\mathbf{y}^k\}_{k=1}^K$
- **Single track:**
 $\mathbf{y}^k = \{\mathbf{y}_t^k\}_{t=1}^{T^k}$
- **Single data point:**
 $\mathbf{y}_t^k = [\bar{s}_x, \bar{s}_y]^\top$
- **Full state:**
 $\mathbf{x}_t^k = [s_x, s_y, v_x, v_y]^\top$
- **Environment influence:**
 $\mathbf{u}_t^k = \mathbf{u}_t^k(\mathbf{s}) = \nabla \mathcal{U}(\mathbf{s}).$

1. Develop a parametrised finite-order model of global $\mathcal{U}(\mathbf{s})$.



Hidden chemoattractant



Time series data:

- **K tracks:** $\mathcal{Y} = \{\mathbf{y}^k\}_{k=1}^K$
- **Single track:**
 $\mathbf{y}^k = \{\mathbf{y}_t^k\}_{t=1}^{T^k}$
- **Single data point:**
 $\mathbf{y}_t^k = [\bar{s}_x, \bar{s}_y]^\top$
- **Full state:**
 $\mathbf{x}_t^k = [s_x, s_y, v_x, v_y]^\top$
- **Environment influence:**
 $\mathbf{u}_t^k = \mathbf{u}_t^k(\mathbf{s}) = \nabla \mathcal{U}(\mathbf{s}).$

1. Develop a parametrised finite-order model of global $\mathcal{U}(s)$.
2. Estimate unobserved $\mathcal{U}(s)$ from localised tracking data \mathcal{Y} .



Defining assumptions

- A migrating cell is moving as a massive Brownian particle:

$$\dot{v}(t) = -\rho v(t) + \sqrt{\sigma} \mathbf{W}(t).$$

- Each cell at each time is moving in response to the acting environment:

$$\dot{v}(t) = -\rho v(t) + \sqrt{\sigma} \mathbf{W}(t) + \psi(t).$$

- Hidden chemoattractant environment is acting on cells as a potential field:

$$\dot{v}(t) = -\rho v(t) + \sqrt{\sigma} \mathbf{W}(t) + \nabla \mathcal{U}(s(t)).$$

- Hidden chemoattractant environment is time-invariant:

$$\mathcal{U}(t) = \text{const.}$$



Defining assumptions

- A migrating cell is moving as a massive Brownian particle:

$$\dot{v}(t) = -\rho v(t) + \sqrt{\sigma} \mathbf{W}(t).$$

- Each cell at each time is moving in response to the acting environment:

$$\dot{v}(t) = -\rho v(t) + \sqrt{\sigma} \mathbf{W}(t) + \psi(t).$$

- Hidden chemoattractant environment is acting on cells as a potential field:

$$\dot{v}(t) = -\rho v(t) + \sqrt{\sigma} \mathbf{W}(t) + \nabla \mathcal{U}(s(t)).$$

- Hidden chemoattractant environment is time-invariant:

$$\mathcal{U}(t) = \text{const.}$$



Defining assumptions

- A migrating cell is moving as a massive Brownian particle:

$$\dot{v}(t) = -\rho v(t) + \sqrt{\sigma} \mathbf{W}(t).$$

- Each cell at each time is moving in response to the acting environment:

$$\dot{v}(t) = -\rho v(t) + \sqrt{\sigma} \mathbf{W}(t) + \psi(t).$$

- Hidden chemoattractant environment is acting on cells as a potential field:

$$\dot{v}(t) = -\rho v(t) + \sqrt{\sigma} \mathbf{W}(t) + \nabla \mathcal{U}(s(t)).$$

- Hidden chemoattractant environment is time-invariant:

$$\mathcal{U}(t) = \text{const.}$$



Defining assumptions

- A migrating cell is moving as a massive Brownian particle:

$$\dot{v}(t) = -\rho v(t) + \sqrt{\sigma} \mathbf{W}(t).$$

- Each cell at each time is moving in response to the acting environment:

$$\dot{v}(t) = -\rho v(t) + \sqrt{\sigma} \mathbf{W}(t) + \psi(t).$$

- Hidden chemoattractant environment is acting on cells as a potential field:

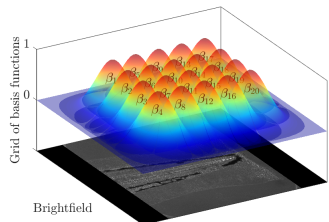
$$\dot{v}(t) = -\rho v(t) + \sqrt{\sigma} \mathbf{W}(t) + \nabla \mathcal{U}(s(t)).$$

- Hidden chemoattractant environment is time-invariant:

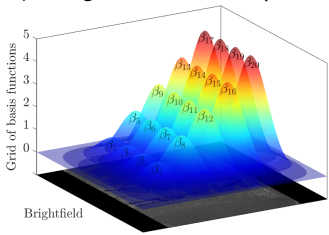
$$\mathcal{U}(t) = \text{const.}$$



Decomposition of the environment



a) 5x4 grid of tensor B-splines



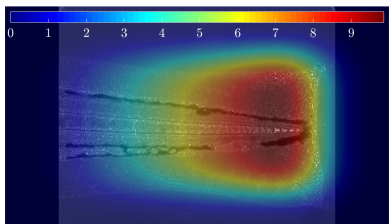
b) θ_h defines magnitude of $\beta_h(s_x, s_y)$

$$\mathcal{U}(s_x, s_y) = \mathcal{B}\Theta = \sum_{h=1}^{N_b} \beta_h(s_x, s_y)\theta_h,$$

$$\Theta = [\theta_1, \dots, \theta_h, \dots, \theta_{N_b}]^\top,$$

$$\mathcal{B} = [\beta_1, \dots, \beta_h, \dots, \beta_{N_b}],$$

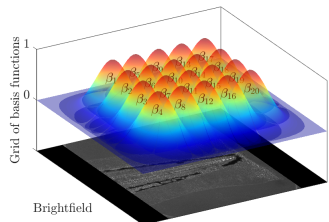
$$\beta_h(s_x, s_y) = \beta_l^4(s_x)\beta_m^4(s_y).$$



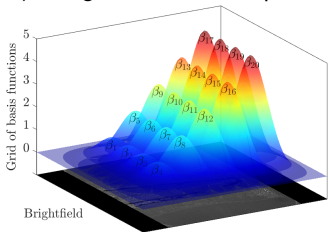
Example of the resultant field.



Decomposition of the environment



a) 5x4 grid of tensor B-splines



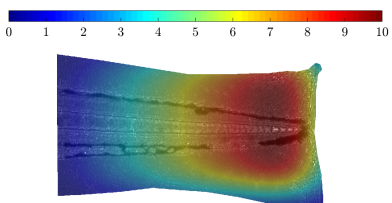
b) θ_h defines magnitude of $\beta_h(s_x, s_y)$

$$\mathcal{U}(s_x, s_y) = \mathcal{B}\Theta = \sum_{h=1}^{N_b} \beta_h(s_x, s_y)\theta_h,$$

$$\Theta = [\theta_1, \dots, \theta_h, \dots, \theta_{N_b}]^\top,$$

$$\mathcal{B} = [\beta_1, \dots, \beta_h, \dots, \beta_{N_b}],$$

$$\beta_h(s_x, s_y) = \beta_l^4(s_x)\beta_m^4(s_y).$$



Example of the resultant field.



Model of neutrophil dynamics

Discrete time SSM of the k-th cell :

$$\boldsymbol{x}_t^k = A\boldsymbol{x}_{t-1}^k + B\phi_{t-1}^k(s_x, s_y)\Theta + G\boldsymbol{w}_{t-1}^k, \quad \boldsymbol{w}_t^k \sim \mathcal{N}(0, Q)$$

$$\boldsymbol{y}_t^k = C\boldsymbol{x}_t^k + \boldsymbol{v}_t^k, \quad \boldsymbol{v}_t^k \sim \mathcal{N}(0, R)$$

where

$$\phi_t^k(s_x, s_y) = \nabla \mathcal{B}(s_x, s_y) = \begin{bmatrix} \frac{\partial \beta_1(s_x, s_y)}{\partial s_x} & \dots & \frac{\partial \beta_h(s_x, s_y)}{\partial s_x} & \dots & \frac{\partial \beta_{N_b}(s_x, s_y)}{\partial s_x} \\ \frac{\partial \beta_1(s_x, s_y)}{\partial s_y} & \dots & \frac{\partial \beta_h(s_x, s_y)}{\partial s_y} & \dots & \frac{\partial \beta_{N_b}(s_x, s_y)}{\partial s_y} \end{bmatrix}.$$

$$A = \begin{bmatrix} \mathbb{I} & T\mathbb{I} \\ \mathbb{O} & (1 - T\rho)\mathbb{I} \end{bmatrix}; B = \begin{bmatrix} \mathbb{O} \\ T\mathbb{I} \end{bmatrix}; G = \begin{bmatrix} \mathbb{O} \\ T\mathbb{I} \end{bmatrix}; C = [\mathbb{I} \quad \mathbb{O}].$$

SMM is linear in Θ and non-linear in \boldsymbol{x} .



Approximate ML estimation

E-step:

$$\mathcal{Q}(\Theta, \hat{\Theta}^i) = \mathbb{E} [\log p(\Theta | \mathcal{Y})] = \mathbb{E} \left[\sum_{k=1}^K \sum_{t=1}^{T_k} \log p(\mathbf{x}_t^k | \mathbf{x}_{t-1}^k, \Theta) | \mathcal{Y}, \hat{\Theta}^i \right] + c.$$

$$p(\mathbf{x}_t^k | \mathbf{x}_{t-1}^k, \Theta) = \mathcal{N}\left((G)^\dagger \left\{ \mathbf{x}_t^k - A\mathbf{x}_{t-1}^k - B\phi(C\mathbf{x}_{t-1}^k)\Theta \right\}, \Sigma_w^{-1}\right).$$

Forecasting step:

$$\mathbf{s}_t^k = C\hat{\mathbf{x}}_{t|T^k}^k, \quad t = 1, \dots, T^k, k = 1, \dots, K.$$

$$\begin{aligned} p(\mathbf{x}_t^k | \mathbf{x}_{t-1}^k, \Theta) &\approx p(\mathbf{x}_t^k | \mathbf{x}_{t-1}^k, \mathbf{s}_{t-1}^k, \Theta) \\ &= \mathcal{N}\left((G)^\dagger \left\{ \mathbf{x}_t^k - A\mathbf{x}_{t-1}^k - B\phi(\mathbf{s}_{t-1}^k)\Theta \right\}, \Sigma_w\right). \end{aligned}$$

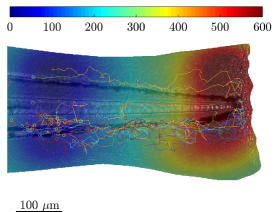
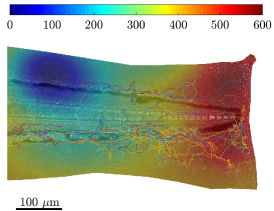
M-step:

$$\hat{\Theta}^{i+1} = \arg \max_{\Theta} \tilde{\mathcal{Q}}(\Theta, \hat{\Theta}^i).$$

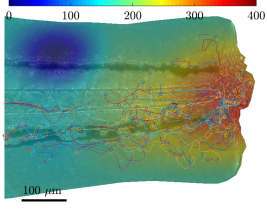
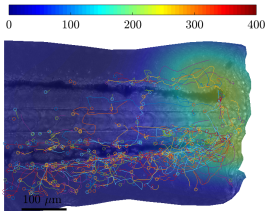
$${}^1\Sigma_w \triangleq \{(G)^\dagger\}^\top (Q_\omega)^{-1}(G)^\dagger$$



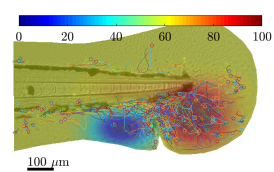
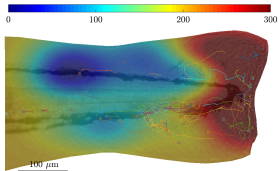
Inferred chemoattractant concentration



a) normal injury
(6 datasets)



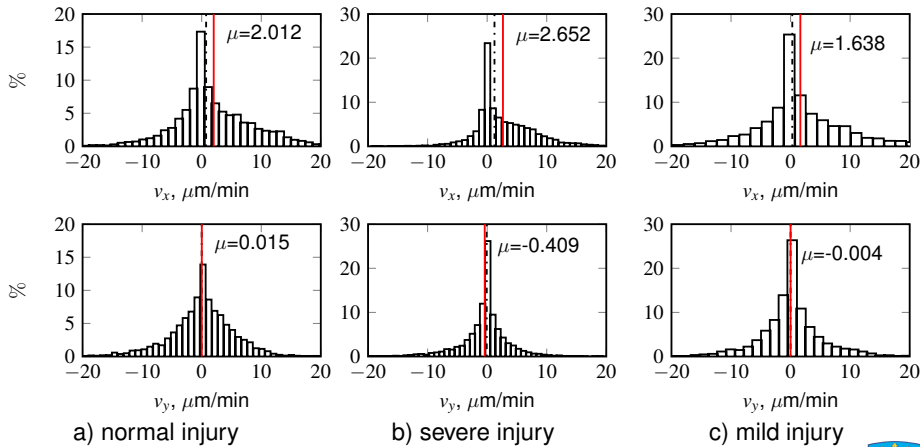
b) severe injury
(2 datasets)



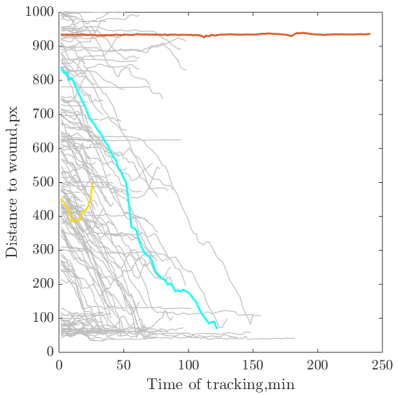
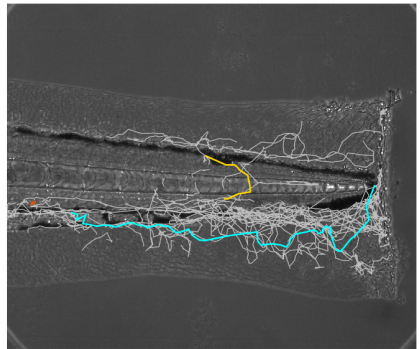
c) mild injury
(6 datasets)



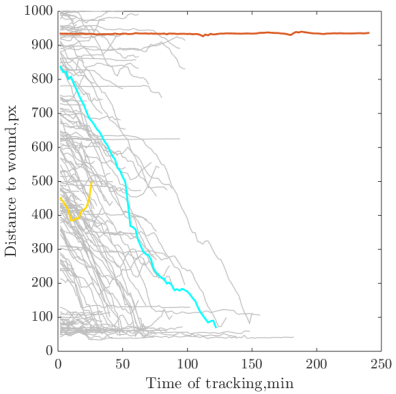
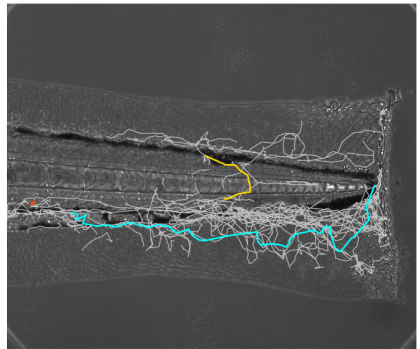
Estimated cell velocities



Heterogeneous cell behaviour



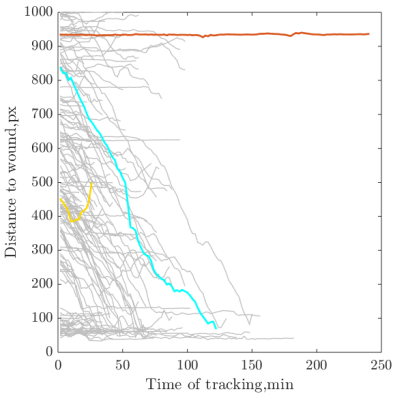
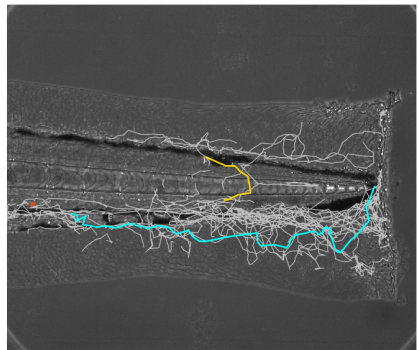
Heterogeneous cell behaviour



1. Determine whether a cell at a given time interacts with the environment $\mathcal{U}(s)$.



Heterogeneous cell behaviour



1. Determine whether a cell at a given time interacts with the environment $\mathcal{U}(s)$.
2. Estimate unobserved $\mathcal{U}(s)$ from the interaction with responsive cells



Defining assumptions (upd.)

Remain the same:

- Each migrating cell is moving as a massive Brownian particle.
- Hidden chemoattractant environment is acting on migrating cells as a potential field.
- Hidden chemoattractant environment is time-invariant.

Relaxed assumptions:

- Each migrating cell at any time can be in one of free modes: stationary, responsive or non-responsive.
- Switching between modes happens randomly.
- Each behavioural mode can be reached from any other mode.



Jump Markov system

$$\begin{aligned} \mathbf{x}_t^k &= A(\mathbf{m}_t^k) \mathbf{x}_{t-1}^k + B(\mathbf{m}_t^k) \phi_{t-1}^k(s_x, s_y) \Theta + G(\mathbf{m}_t^k) \mathbf{w}_{t-1}^k, \\ \mathbf{w}_t^k &\sim \mathcal{N}(0, Q(\mathbf{m}_t^k)), \\ \mathbf{m}_t^k &\in \{M^1, M^2, M^3\}. \end{aligned}$$

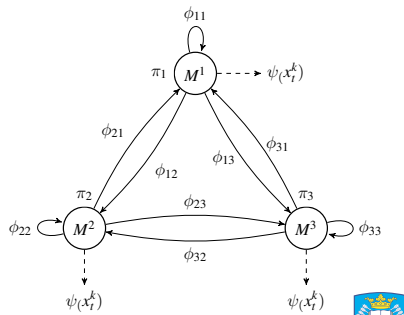
Cell modes:

$$M^1 : A = \begin{bmatrix} \mathbb{I} & T\mathbb{I} \\ \mathbb{O} & (1 - T\rho(M^1))\mathbb{I} \end{bmatrix} B = \begin{bmatrix} \mathbb{O} \\ T\mathbb{I} \end{bmatrix}$$

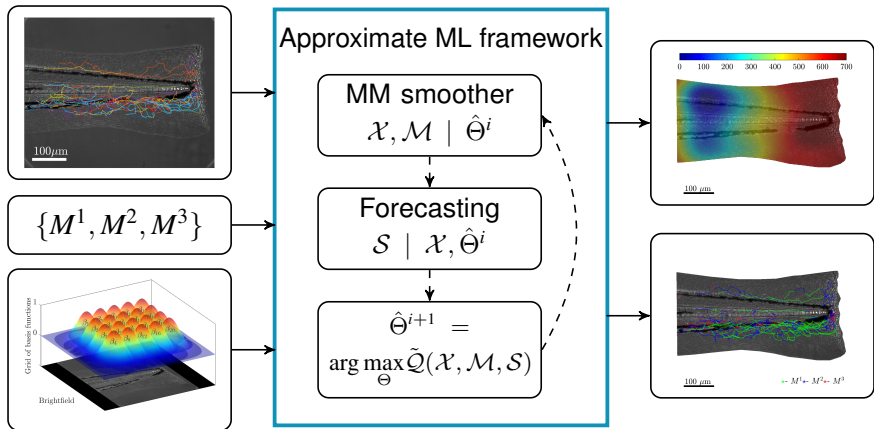
$$M^2 : A = \begin{bmatrix} \mathbb{I} & T\mathbb{I} \\ \mathbb{O} & (1 - T\rho(M^2))\mathbb{I} \end{bmatrix} B = \begin{bmatrix} \mathbb{O} \\ \mathbb{O} \end{bmatrix}$$

$$M^3 : A = \begin{bmatrix} \mathbb{I} & T\mathbb{I} \\ \mathbb{O} & (1 - T\rho(M^3))\mathbb{I} \end{bmatrix} B = \begin{bmatrix} \mathbb{O} \\ \mathbb{O} \end{bmatrix}$$

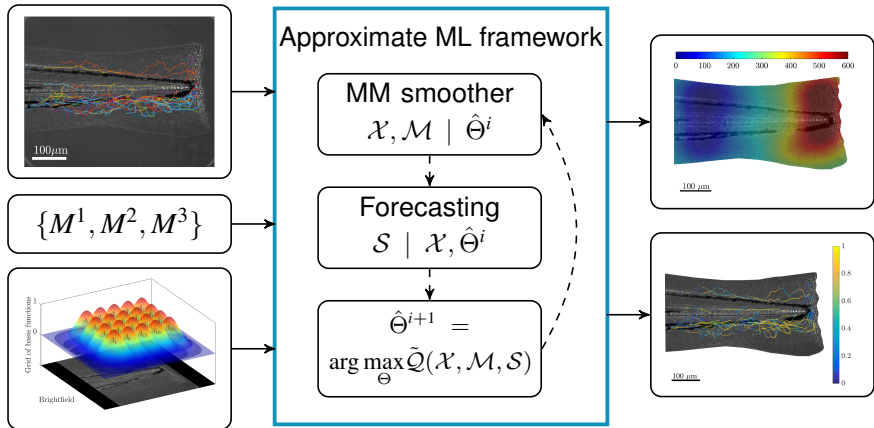
$$Q(M^3) \ll Q(M^1) < Q(M^2).$$



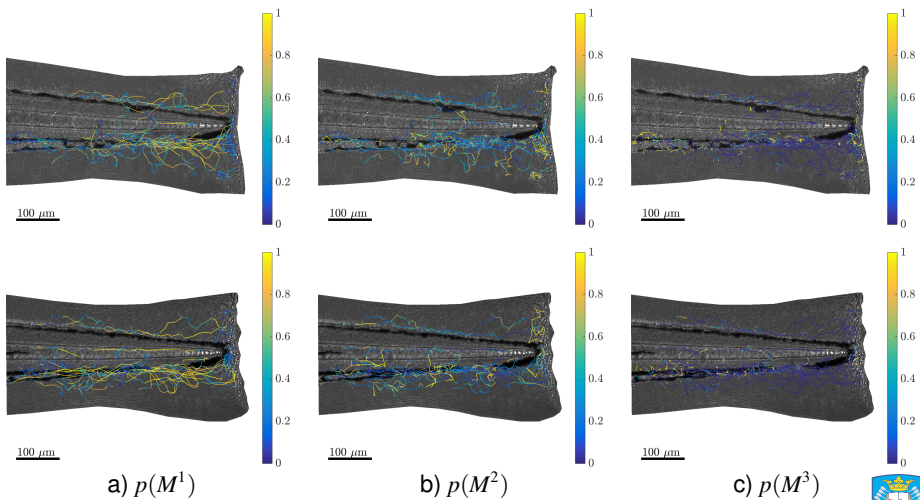
Inference framework



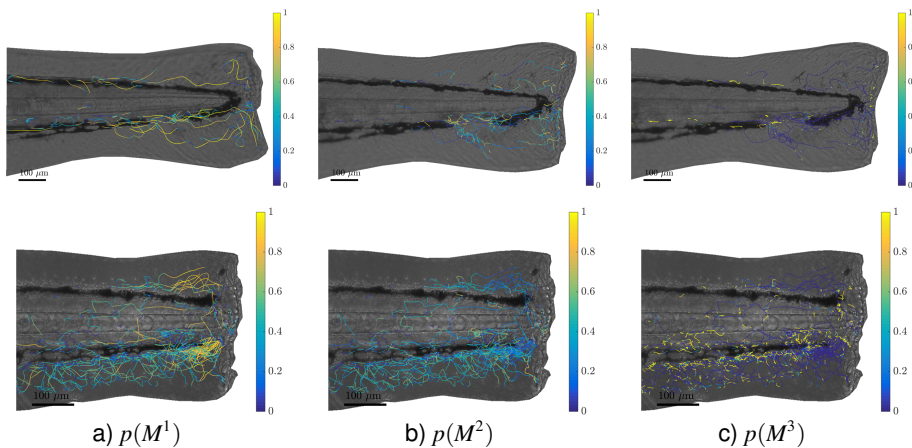
Inference framework



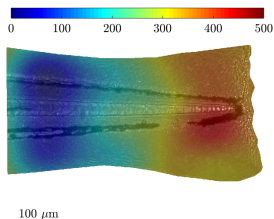
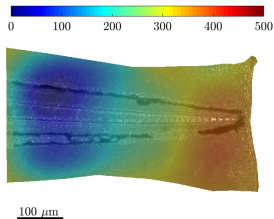
Migratory modes - normal injury



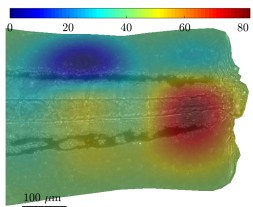
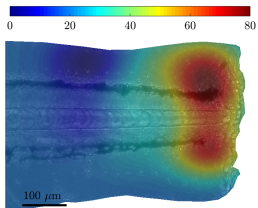
Migratory modes - severe and mild injury



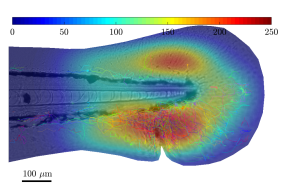
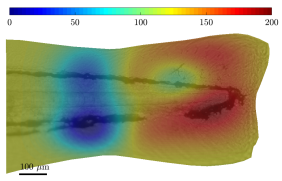
Inferred chemoattractant environment



a) normal injury



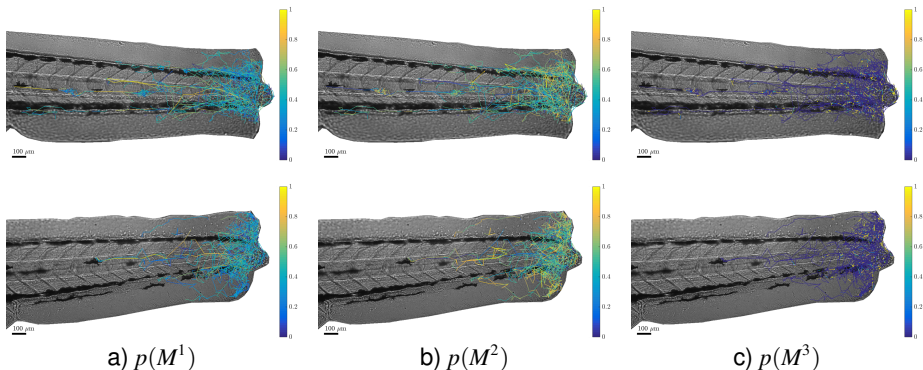
b) severe injury



c) mild injury



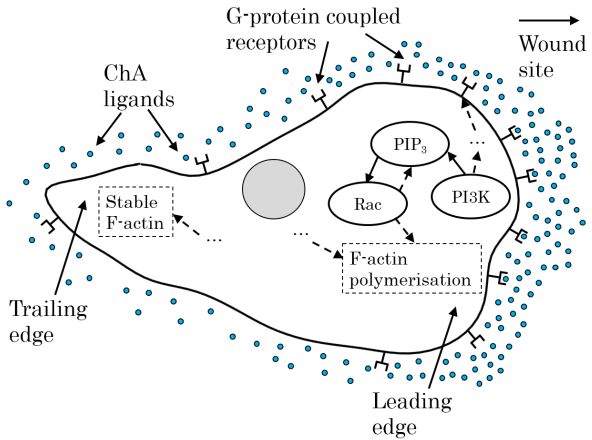
Reverse migration



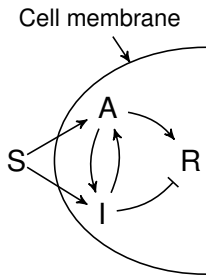
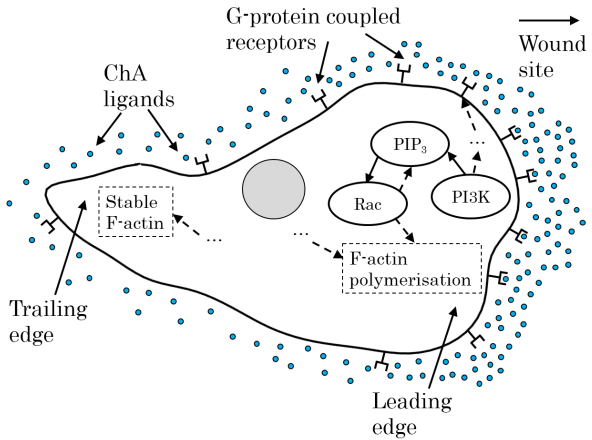
For 4 datasets there is higher probability of neutrophils diffusing away from the wound.



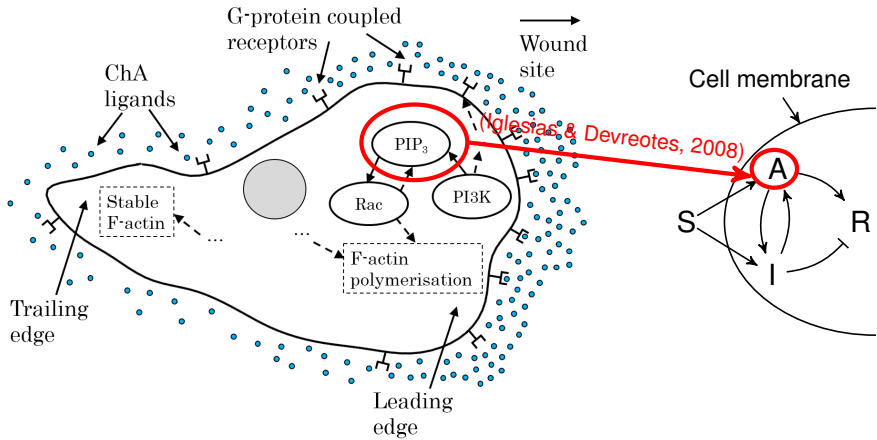
Signal to migration



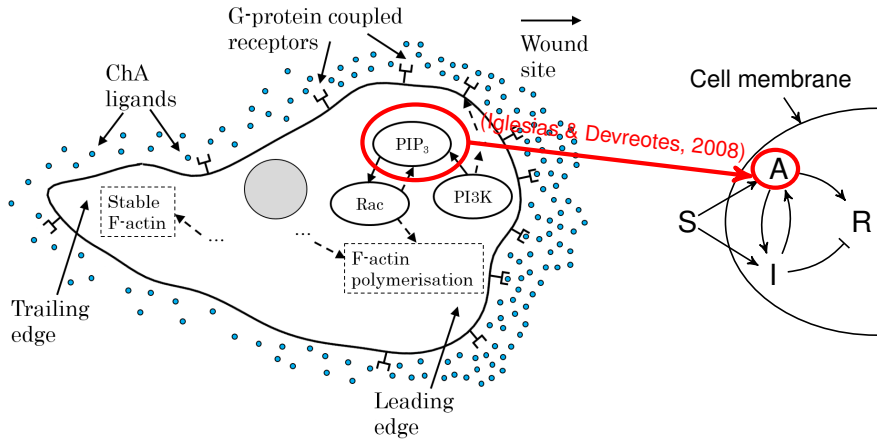
Signal to migration



Signal to migration

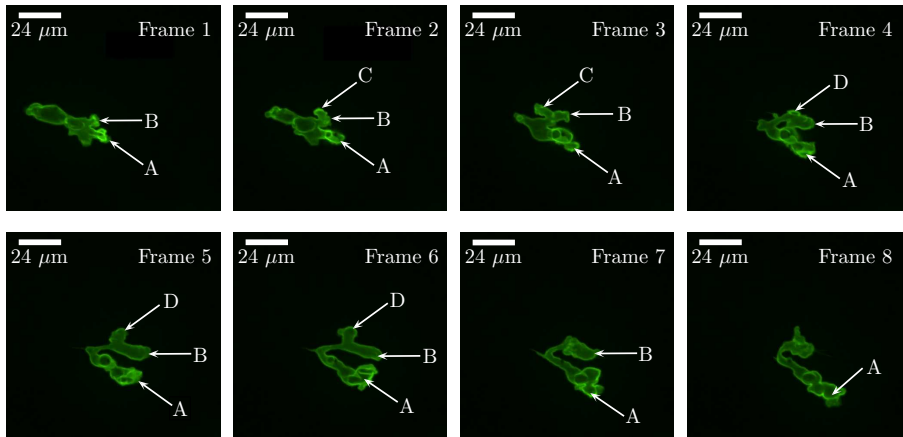


Signal to migration



Does PIP₃ activate pseudopod growth in migrating neutrophils?





Data



Defining assumptions

- PIP₃ is the only activator regulating cell membrane protrusions.
- The integrated fluorescence intensity obtained from the imaging data is proportional to the local PIP₃ concentration.
- The cell is a 2-D curve Γ_t .
- Local shape change is fully described by the evolution of local normal velocity.

$$\mathbf{v}_{t+1}^k = \mathbf{v}_t^k + \frac{1}{m} \mathcal{F} + \mathbf{w}_t.$$



Forces acting on cell boundary

$$\mathcal{F} = (\mathcal{F}_{\text{visc}} + \mathcal{F}_{\text{pro}} + \mathcal{F}_{\text{ten}} + \mathcal{F}_{\text{vol}})\nu,$$

- **Protrusive force** caused by acting regulators along the membrane:

$$\mathcal{F}_{\text{pro}} = \alpha_{\text{pro}} a_t^k.$$

- **Surface tension** prevents cell membrane from stretching:

$$\mathcal{F}_{\text{ten}} = \alpha_{\text{ten}} \kappa_t^k.$$

- **Volume conservation** balances small volume changes:

$$\mathcal{F}_{\text{vol}} = \alpha_{\text{vol}} \Delta A_t.$$

- **Viscous force** opposes cell motion:

$$\mathcal{F}_{\text{visc}} = -\alpha_{\text{vv}} v_t^k.$$



State space model

$$\Gamma_t : s_t^k, \quad k = 1, \dots, K.$$

Local evolution for the node s_t^k :

$$v_{t+1}^k = Av_t^k + Bu_t^k + w_t^k, \quad w_t^k \sim \mathcal{N}(0, Q).$$

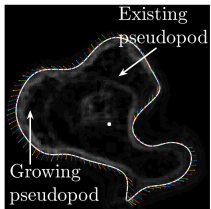
$$y_t^k = Cv_t^k.$$

- $A = 1 - \alpha_{vv}$; $B = [\alpha_{\text{pro}}, \alpha_{\text{ten}}, \alpha_{\text{vol}}]$;
- $u_t^k = [a_t^k, \kappa_t^k, \Delta A_t]^\top$, where
 - a_t^k - local concentration of PIP₃;
 - κ_t^k - local curvature;
 - $\Delta A_t = A_t - A_0$ - change in cell shape.
- $\Theta = \{A, B, Q, v_0, P_0\}$ - estimated via classic EM algorithm.

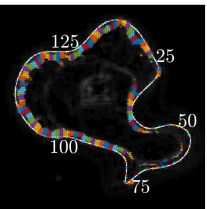


Image processing

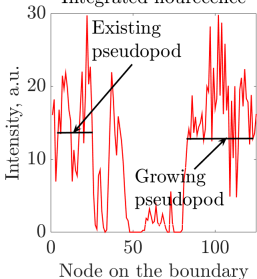
Boundary velocities



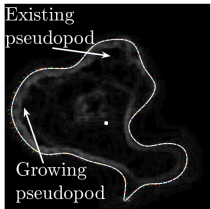
Node associated pixels



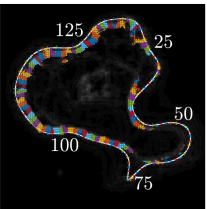
Integrated fluorescence



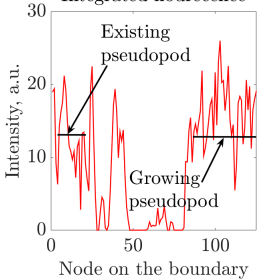
Boundary velocities



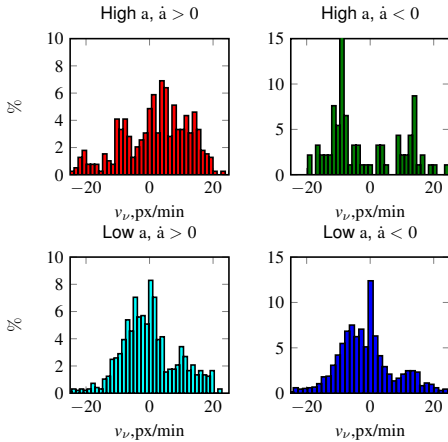
Node associated pixels



Integrated fluorescence



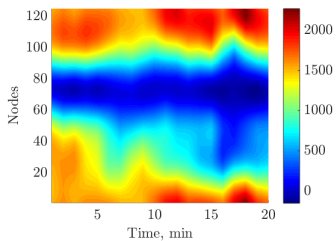
Motile cells observed in vivo



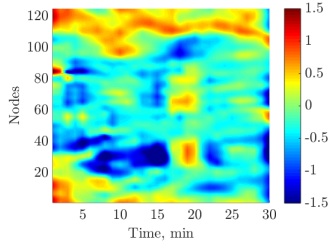
- Very weak correlation between a_{t-1}^k and v_t^k for all cells;
- PIP₃ does not activate protrusion growth;
- Mann-Whitney test results: on average, higher concentrations of PIP₃ accelerate protrusion growth.



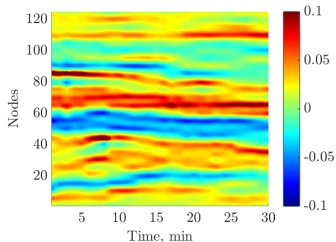
Motile cells observed in vivo



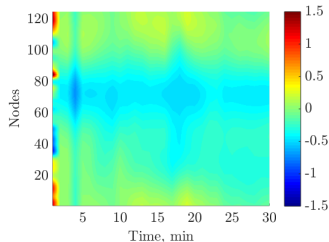
a) Smoothed intensity.



c) Estimated velocity.



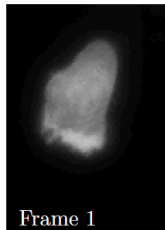
a) Local curvature.



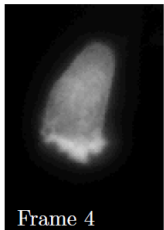
d) Predicted velocity.



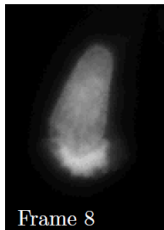
Polarised cell observed in vitro



Frame 1



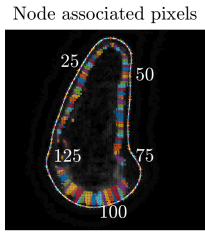
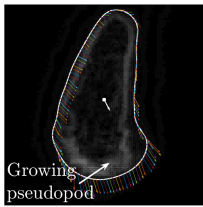
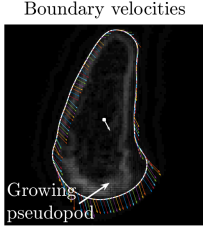
Frame 4



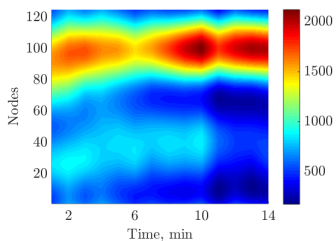
Frame 8



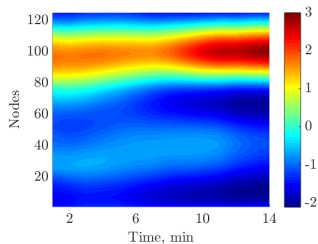
Frame 12



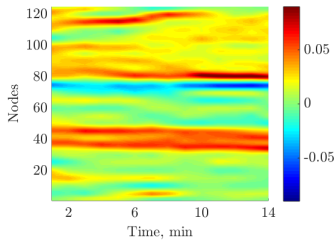
Polarised cell observed in vitro



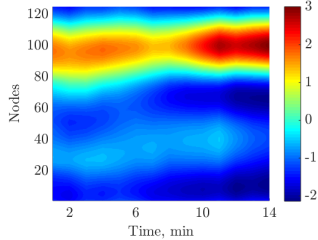
a) Smoothed intensity.



c) Estimated velocity.



a) Local curvature.



d) Predicted velocity.



Technical contributions

- A reconfigurable hybrid model of individual cell dynamics that incorporates the influence of the global environment.
- A statistical framework for simultaneous inference of the global chemoattractant environment and cell behavioural modes.
- An image processing and estimation framework that links local cell boundary evolution to observed subcellular concentrations.



Contributions in field of application

- Investigation of neutrophil-environment interaction on different stages of inflammation.
- Quantitative evidence that the dominant mode of neutrophil reverse migration is random walk.
- Quantitative evidence that PIP_3 does not activate protrusions but accelerates existing leading edges in cells performing chemotaxis.



Future work

- Utilising hierarchical/multi-resolution basis functions in environment decomposition.
- Introducing priors for the field parameters and Bayesian inference.
- Considering time-varying environment for recruitment stage of inflammation.
- Considering competing gradients for resolution stage of inflammation.
- Shorten this presentation.



Disseminated results

- A. Kadochnikova, H.M. Isles, S.A. Renshaw, V. Kadirkamanathan. "Estimation of Hidden Chemoattractant Field from Observed Cell Migration Patterns". A peer-reviewed paper in *Proceedings of 18th IFAC Symposium on System Identification SYSID 2018*.
- H.M. Isles, C. Muir, A. Kadochnikova, C.A. Loynes, V. Kadirkamanathan, P.M. Elks, S.A. Renshaw. "Non-apoptotic pioneer neutrophils initiate a swarming response in a zebrafish tissue injury model" under review in eLife Reports, 2019.

In preparation:

- A. Kadochnikova, V. Kadirkamanathan. "An Approximate Maximum Likelihood Framework for Estimating the Environment Driving multiple objects with Hybrid Dynamics".
- A. Kadochnikova, H.M. Isles, S.A. Renshaw, V. Kadirkamanathan. "Inference of the External Stimuli Environments from Heterogeneous Behaviour of Migrating Neutrophils in Zebrafish Model of Inflammation".



Thank you!
Questions?

